Available online at www.sciencedirect.com
ScienceDirect
Journal of Molecular Catalysis A: Chemical 275 (2007) 130–138
JOURNAL OF MOLECULAR CATALYSIS A: CHEMICAL
www.elsevier.com/locate/molcata

Catalytic behavior of ternary $Cu/ZnO/Al_2O_3$ systems prepared by homogeneous precipitation in water-gas shift reaction

Ikuo Atake [a], Kazufumi Nishida [a], Dalin Li [a], Tetsuya Shishido [b], Yasunori Oumi [a], Tsuneji Sano [a], Katsuomi Takehira [a,*]

[a] *Department of Chemistry and Chemical Engineering, Graduate School of Engineering, Hiroshima University, Kagamiyama 1-4-1, Higashi-Hiroshima 739-8527, Japan*
[b] *Department of Molecular Engineering, Graduate School of Engineering, Kyoto University, Katsura 1, Nishigyo-ku, Kyoto 615-8510, Japan*

Received 7 March 2007; received in revised form 25 May 2007; accepted 26 May 2007
Available online 3 June 2007

Abstract

Ternary $Cu/ZnO/Al_2O_3$ catalysts have been prepared by homogeneous precipitation (*hp*) using urea hydrolysis and tested for the water-gas shift reaction. The Cu/Zn ratio was fixed at 1/1, and the effects of the Al addition on the precipitation procedure, the precursor structure and the catalytic activity have been studied.

The precipitation proceeded stepwise; Cu(II) nitrate was first hydrolyzed, followed by the hydrolysis of Zn(II) nitrate, but the final compounds consist mainly of aurichalcite. It is likely that amorophous $Cu(OH)_2$ formed first was converted to aurichalcite *via* a dissolution-reprecipitation mechanism assisted by Zn(II). A significant leaching of Cu took place with increasing Al content during the precipitation at 90 °C. The Cu leaching was effectively suppressed by lowering the temperature to 80 °C, but resulting in a slight decrease in the catalytic activity. In the *hp*-catalyst precursors, aurichalcite was always observed as the main component, whereas hydrotalcite and malachite appeared with increasing Al component. The catalytic activity increased by the addition of 5 mol% of Al and decreased with further addition of Al. The activity apparently depended on the Cu metal surface area on the catalyst, but the turn over frequency calculated based on the surface Cu metal significantly varied depending on the Al content. Moreover, the intensity of the reduction peak around 225 °C assigned to $Cu^{2+} \rightarrow Cu^{+}$ in the TPR well correlated with the catalytic activity. It is suggested that Cu/Zn bimetallic aurichalcite has an important role as the catalyst precursor and the reduction–oxidation between Cu^{+} and Cu^{0} plays in the catalytic mechanism of the shift reaction.
© 2007 Published by Elsevier B.V.

Keywords: Water-gas shift reaction; $Cu/ZnO/Al_2O_3$ catalyst; Aurichalcite; Homogeneous precipitation; Cu^{+} active species

1. Introduction

The water-gas shift reaction is mostly used in the production of hydrogen *via* the steam reforming of hydrocarbons and is of importance for future energy technologies such as fuel cells. Polymer electrolyte fuel cells (PEFC) have been extensively studied due to their attractive properties, such as high power density, low emissions of NO*x*, dust, noise, etc., low temperature operation and compactness [1,2]. In this system, hydrogen is used as a fuel; it is supplied from steam reforming of hydrocarbons such as methane, propane and kerosene. The problem is that the reformed gas contains CO at the level of 1–10% which adsorbs irreversibly on the Pt electrode of the PEFC at the operating temperature (ca. 80 °C) and hinders the electrochemical reaction [3,4]. Therefore, CO must be removed from the reformed gases to less than 10–20 ppm before feeding the gas mixture to the Pt electrode. The water-gas shift reaction is desirable for removal of a large amount of CO since it is moderately exothermic reaction ($\Delta H_{298} = -41.1\ \mathrm{kJ\,mol^{-1}}$) and the reaction temperature is easy to control. The equilibrium conversion of CO is dependent largely on the reaction temperature: since the shift reaction is an exothermic reaction, lower temperature is favored for higher CO removal. On the other hand, from the viewpoint of reaction kinetics, the reactant gases are not active enough to reach the chemical equilibrium at low temperature.

* Corresponding author. Tel.: +81 82 424 6488: fax: +81 82 424 6488.
E-mail address: takehira@hiroshima-u.ac.jp (K. Takehira).

1381-1169/$ – see front matter © 2007 Published by Elsevier B.V.
doi:10.1016/j.molcata.2007.05.040

Ternary $Cu/ZnO/Al_2O_3$ catalysts have been widely employed commercially since the early 1960s in the water-gas shift reaction; the catalyst was usually prepared by co-precipitation method to afford the higher Cu metal dispersion in the resulting catalyst and, as a consequence, the higher catalytic activity [5]. Various Cu catalysts have been prepared according to various techniques and tested in the shift reaction. Co-precipitated $Cu/ZnO/Al_2O_3$ catalysts were more sustainable than the impregnated catalysts in the shift reaction [6]. However impregnation of CeO_2 on Cu–Zn precursor before calcination was useful for stabilizing the Cu/ZnO catalyst against the shift reaction [7]. High activity was obtained by the formation of spinel type Cu–Al–Zn oxides giving rise to fine Cu particles deposited on the support [8], on which oxygen assisted the shift reaction [9]. The Cu–Al–Zn oxides catalyst is unstable and gave rise to the sintering of Cu at high temperature, whereas stable spinel $CuAl_2O_4$ structure was moderately active in the shift reaction [10–12]. Interestingly, spinel $CuMn_2O_4$ and moreover nonstoichiometric Cu/MnO catalysts showed high activity as well as high durability in the shift reaction [12].

We have prepared Cu/ZnO catalysts by homogeneous precipitation (*hp*) using urea hydrolysis; the catalysts showed higher activity than those prepared by co-precipitation (*cp*) for hydrogen production by steam reforming of methanol [13]. The *hp*-catalysts were mainly derived from aurichalcite as the precursor, and both morphology and crystallinity of the precursors revealed an important role in the catalytic activity. The *hp*-Cu/ZnO catalysts showed also high activity for the shift reaction [14] and moreover the addition of small amount of Mg enhanced the activity of the *hp*-Cu/ZnO catalysts [15]. Aurichalcite contains both Cu and Zn closely located each other in the structure and therefore affords highly dispersed Cu metal species possessing a good contact with ZnO particles after the calcination, followed by the reduction, resulting in the formation of Cu^+ proposed as the active species [14,15]. Actually ternary $Cu/ZnO/Al_2O_3$ catalysts have been used in the shift reaction in the reformer. Aurichalcite is composed of the Cu/Zn binary system and unable to contain Al component in the crystal structure. Moreover Cu^{2+} ions can be depleted by ammonia originating from urea hydrolysis during the *hp*-preparation [16]. In the present work, we have prepared *hp*-Cu/Zn/Al catalysts by urea hydrolysis, and investigated on the effect of the Al component on the precipitation procedure, on the structure of the catalyst precursors and further on the activity for the shift reaction.

2. Experimental

2.1. Preparation of the catalysts

Ternary $Cu/ZnO/Al_2O_3$ catalysts were prepared by homogeneous precipitation using urea hydrolysis [17–19]. An excess amount of urea was dissolved in an aqueous solution of corresponding metal nitrates at room temperature. Typically, each 0.0160 mol of $Cu(NO_3)_2{\cdot}3H_2O$ and $Zn(NO_3)_2{\cdot}6H_2O$, 0.00356 mol of $Al(NO_3)_3{\cdot}9H_2O$ and 0.711 mol of urea were dissolved in 500 ml of distilled water for the preparation of the *hp*-$Cu/ZnO/Al_2O_3$ catalyst of 10 mol% of the Al content. The urea was hydrolyzed by heating the mixture at 80 or 90 °C for 24–36 h. During the hydrolysis of urea, hydroxide ions are generated in the homogeneous solution (Eq. (1)), which hydrolysed

$$CO(NH_2)_2 + H_2O \rightarrow 2NH_4{}^+ + HCO_3{}^- + OH^- \quad (1)$$

metal nitrates to the corresponding hydroxides and finally to the hydroxycarbonates as the catalyst precursors. It is expected that the higher homogeneity of the precipitate will be attained by the *hp*-method than by the *cp*-method, since there is theoretically no gradient in the concentration of precipitants due to its *in situ* formation in the homogeneous solution in the *hp*-method. The precipitates were then filtered, washed with distilled water, dried at 80 °C and finally calcined at 300 °C for 3 h in air.

Ternary *cp*-$Cu/ZnO/Al_2O_3$ catalysts were prepared as reference by co-precipitation starting from metal nitrates in Na_2CO_3 aqueous solution at pH 9.0 controlled by NaOH aqueous solution.

The precursors of the *hp*-$Cu/ZnO/Al_2O_3$ catalysts were also prepared without stirring, *i.e.*, under the thermal convection, at 90 °C during the heating of the solution. The reservoir for the precipitation was heated by immersing it in the oil bath controlled at 90 °C.

2.2. Characterization of the catalysts

The structure of the catalysts has been studied by using XRD, SEM, ICP, TPR, N_2O decomposition and N_2 adsorption methods.

Powder X-ray diffraction was recorded on a Rigaku powder diffraction unit, RINT 2250VHF, with mono-chromatized Cu Kα radiation (λ = 0.154 nm) at 40 kV and 30 mA. The diffraction pattern was identified by comparing with those included in the JCPDS (Joint Committee of Powder Diffraction Standards) data base.

Scanning electron microscope (SEM) measurements were performed with a JEOL JEM-6320F microscope by using a Noran Voyager energy dispersive X-ray spectroscopy at an accelerating voltage of 300 kV.

Inductively coupled plasma (ICP) optical emission spectrometry was used for the determination of the metal content in each sample synthesized above. The measurements were performed with a Seiko SPS 7700, and the sample was dissolved in a mixture of HF and HNO_3 acids before the measurements.

Temperature-programmed reduction (TPR) of the catalyst was performed at a ramping rate of 10 °C min^{-1} from ambient temperature to 500 °C using a mixture of 5 vol% H_2/Ar as reducing gas after passing through a 13× molecular sieve trap to remove water. A U-shaped quartz tube reactor, the inner diameter of which was 6 mm, equipped with a TCD for monitoring the H_2 consumption was used. Prior to the TPR measurement, 50 mg of sample was calcined at 300 °C for 1.5 h in O_2/Ar (10/40 ml min^{-1}) mixed gas flow.

The copper metal surface areas were determined by the N_2O decomposition method at 90 °C as reported by Evans et al. [20], assuming a reaction stoichiometry of two Cu atoms per oxygen atom and a Cu surface density of 1.63×10^{19} Cu atom m^{-2}. Prior

to the measurement, 150 mg of sample was reduced at 200 °C for 0.5 h in H_2/N_2 (5/30 ml min^{-1}) mixed gas flow.

N_2 adsorption (−196 °C) study was used to obtain BET surface area of the samples after the calcination. The measurement was carried out on a Bell-Japan Belsorp-mini. The samples were pretreated in N_2 at 200 °C for 10 h before the measurements.

2.3. Catalytic reactions and analyses of the products

The water-gas shift reaction was carried out using a fixed bed reactor at atmospheric pressure. A U-shaped Pyrex glass tube with inner diameter of 8 mm was used as a reactor. Typically 100 mg of catalyst, which has been pelletized and sieved to 0.25–0.42 mm in diameter, was loaded into the reactor together with 200 mg of quartz beads. The catalyst was treated in a mixed gas flow of H_2/N_2 (5/30 ml min^{-1}) at 200 °C for 30 min and then purged with N_2 (purity, 99.99%). The reaction was started by introducing a gas mixture to the reactor; the composition was chosen supposing the products after the steam reforming reaction at 700 °C. Typically mixed gas flow of $CO/H_2O/H_2/CO_2/N_2$ (0.77/2.2/4.46/0.57/30 ml min^{-1}) was supplied for the reaction, where N_2 was used as the internal standard for the calculations of the conversions of CO and H_2O. Each gas flow was regulated by a mass-flow controller, and H_2O was fed through a micro-feeder Shimadzu LC 20AD. Gases and H_2O were mixed in the reservoir located just before the reactor and kept at desired temperature.

The products were automatically analyzed by on-line gas chromatographs (GC). A GC with packed Porapak N column (2 m, 1/4 i.d.), He carrier gas and TCD were used to analyze N_2 and H_2O. Another GC with packed Porapak Q column (3 m, 1/4 i.d.) and molecular sieves 5A column (2 m, 1/4 i.d.) in a series, Ar carrier gas and TCD were used to analyze H_2, N_2 and CO. CO_2 and H_2O were also quantified by another GC with TCD using a packed Porapak N column (1 m, 1/4 i.d.), Porapak Q column (2 m, 1/4 i.d.) and molecular sieves 5A column (2 m, 1/4 i.d.) in a series. All the lines and valves through the water feed, the reactor, the exit and the gas chromatographs were heated to 150 °C to prevent the condensation of water.

3. Results and discussion

3.1. Structure of the hp-Cu/ZnO/Al_2O_3 catalysts

Fig. 1A and B shows the XRD patterns of the *hp*-Cu/ZnO/Al_2O_3 catalyst precursors as synthesized by precipitation, followed by aging, *i.e.*, heating at 90 °C and at 80 °C, respectively. Three types of hydroxycarbonates, *i.e.*, aurichalcite $(Cu,Zn)_5(CO_3)_2(OH)_6$, hydrotalclie $(Cu,Zn)_6Al_2(OH)_{16}CO_3{\cdot}4H_2O$, and malachite $Cu_2(CO_3)(OH)_2$ were formed. In both cases at 80 and 90 °C, aurichalcite was observed as a main phase; with increasing Al content, the reflection lines of aurichalcite were weakened, whereas those of hydrotalcite were strengthened. The reflections of malachite appeared together with an unidentified reflection, and their intensities were stronger at 80 °C than at 90 °C, indicating that 90 °C is preferable for the selective formation of aurichalcite. After the calcination at 300 °C for 3 h, all hydroxycarbonates in the

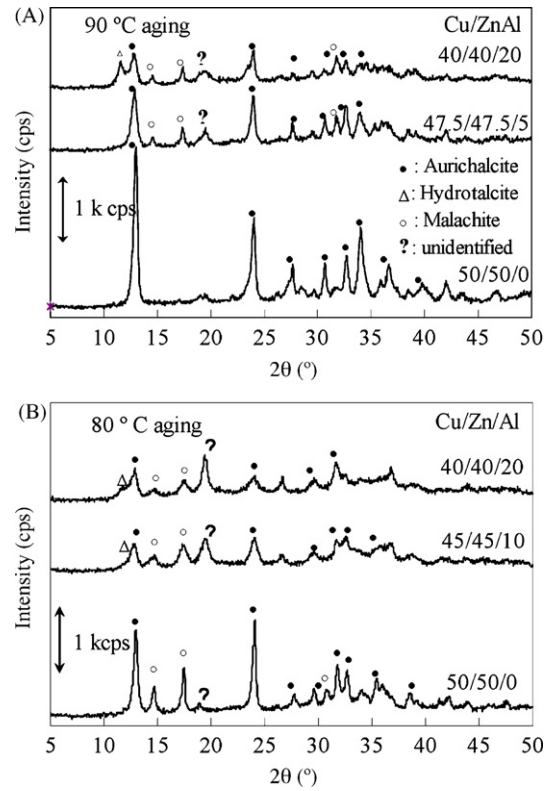

Fig. 1. XRD patterns of the precursors of the *hp*-Cu/ZnO/Al_2O_3 catalysts as deposited by aging at 90 °C (A) and at 80 °C (B). (●) Aurichalcite $(Cu,Zn)_5(CO_3)_2(OH)_{16}$; (△) hydrotaclite $(Cu,Zn)_6Al_2(OH)_{16}CO_3{\cdot}4H_2O$; (◯) malachite $Cu_2(CO_3)(OH)_2$; (?) not assigned.

precursors were decomposed and the reflection lines of both CuO and ZnO appeared (Fig. 2A). With increasing Al content, these lines became broadened and feeble, suggesting that both CuO and ZnO particles were dispersed by the addition of Al component. The particle size of ZnO was calculated at 4.8 and

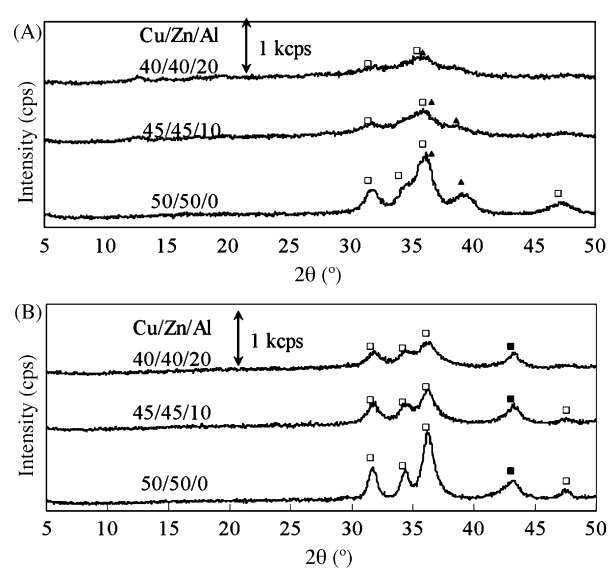

Fig. 2. XRD patterns of the *hp*-Cu/ZnO/Al_2O_3 catalysts after the cacination (A) and after the reaction (B). The catalysts were prepared by aging at 90 °C. (□) ZnO; (▲) CuO; (■) Cu metal.

Table 1
Physico-chemical properties of *hp*-Cu/ZnO/Al_2O_3 catalysts

Catalyst (Cu/Zn/Al atomic ratio)[a]	Cu/Zn/Al composition[b]	Surface (area/m^2 g_{cat}^{-1})[c]	Cu metal surface (area/m^2 g_{cat}^{-1})[d]
hp-Cu/Zn/Al (50/50/0)	51.9/48.1/0	79.7	48.8
hp-Cu/Zn/Al (47.5/47.5/5)	48.0/47.3/4.7	69.8	52.0
hp-Cu/Zn/Al (45/45/10)	45.5/45.2/9.3	63.1	46.1
hp-Cu/Zn/Al (42.5/42.5/15)	41.1/43.8/15.1	74.4	39.8
hp-Cu/Zn/Al (40/40/20)	38.5/41.0/20.5	75.1	44.8
hp-Cu/Zn/Al (50/50/0)*	49.2/50.8/0	80.9	37.2
hp-Cu/Zn/Al (45/45/10)*	45.5/43.4/11.1	68.2	30.6
hp-Cu/Zn/Al (40/40/20)*	41.0/38.5/20.5	66.4	24.0

[a] Catalysts were prepared by the *hp*-method aged at 90 °C (*80 °C) using the raw materials of the Cu/Zn/Al metal compositions shown in the parentheses.
[b] Obtained by the ICP method.
[c] Obtained by the N_2 adsorption.
[d] Obtained by the N_2O pulse method.

3.8 nm for the Cu/Zn/Al composition (50/50/0) and (45/45/10), respectively, whereas that of CuO was at 6.1 nm for (50/50/0). The reflection lines were too weak to calculate the particle size for the other samples. After the reaction at increasing reaction temperature from 150 to 300 °C for 6 h, the particle size of ZnO increased to 8.1, 5.8 and 4.4 nm for the Cu/Zn/Al composition (50/50/0), (45/45/10) and (40/40/20), respectively, whereas that of Cu metal was 7.1, 6.6 and 6.7 nm for (50/50/0), (45/45/10) and (40/40/20), respectively. It is concluded that the Al component worked against the sintering, *i.e.*, the crystal growth, of ZnO and Cu species.

BET surface area and Cu metal surface area of the *hp*-catalysts after the calcination are shown in Table 1, together with the Cu/Zn/Al metal compositions obtained by the ICP analyses. At 90 °C, BET surface area first decreased with increasing Al content to 10%, and increased with further increase in the Al content, whereas the Cu metal surface area first increased and decreased with increasing Al content. On the other hand, both surface areas of the Cu/Zn/Al samples aged at 80 °C were almost lower than those aged at 90 °C and decreased with increasing Al content.

The results of TPR measurements of the *hp*-Cu/Zn/Al catalysts prepared by aging at 90 °C are shown in Fig. 3. The catalysts were pre-reduced at 200 °C before the TPR measurements considering the conditions for testing the catalytic activity. The reduction peak appeared mainly at 225 °C together with a weak shoulder around 201 °C for the samples of low Al contents. By the addition of Al, the former peak was weakened and the shoulder disappeared, whereas new peaks appeared at 248 and 276 °C. Both peaks were enhanced with increasing Al content. The curves obtained for *cp*-Cu/ZnO (50/50) and *cp*-Cu/ZnO/Al_2O_3 (40/40/20) prepared by co-precipitation at pH 9.0 with NaOH as the pH controller are shown in Fig. 3 as references. Although the peak around 225 °C was observed for the *cp*-Cu/ZnO (50/50), a big shoulder appeared around 250 °C and the reduction peaks appeared at the higher temperatures compared with *hp*-Cu/ZnO/Al_2O_3. The highest peak temperature observed for *hp*-Cu/ZnO/Al_2O_3 with the high Al contents, 276 °C, was lower compared to that observed above 300 °C for *cp*-Cu/ZnO/Al_2O_3 as reference. The peak at 225 °C remained always as the main peak irrespective of the Al content for *hp*-Cu/ZnO/Al_2O_3 catalysts.

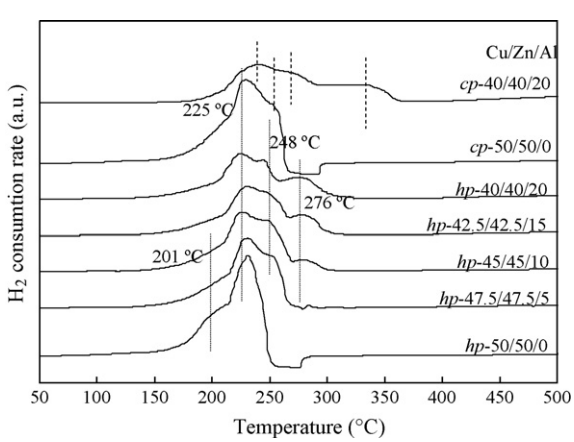

Fig. 3. TPR profiles of the *hp*-Cu/ZnO/Al_2O_3 catalysts with varying Al contents. *cp*-Cu/ZnO/Al_2O_3 catalysts as reference were prepared by precipitation at pH 9.0 with NaOH as the pH controller.

3.2. Hydrolysis of Cu and Zn during the precipitation

During the precipitation at 90 °C, the pH of the solution rather quickly increased from 4.0 to 8.0 within 10 h, followed by a gradual increase and finally reached the equilibrium value around 8.5 at 24 h of aging (Fig. 4). The pH variation during the precipitation was scarcely affected by the Al content between 0 and 20 mol%. The pH changes showed a breaking point around pH 6.0, suggesting that the precipitation proceeded in two successive steps; the first one took place within 2–3 h aging and the second step started when pH rose to 6. It is likely that the first and the second correspond to the precipitations of copper and zinc, respectively [18]. This two-step precipitation is a consequence of the dissimilar hydrolytic properties of Cu(II) and Zn(II), the d^9 Cu^{2+} ion being more acidic than the d^{10} Zn^{2+} ion and first hydrolyzed to form amorphous copper hydroxide (*am*-$Cu(OH)_2$) [21]. Although the initial precipitation stage is different for each Cu(II) and Zn(II), the subsequent evolution of *am*-$Cu(OH)_2$ is strongly affected by the presence of Zn(II); *am*-$Cu(OH)_2$ evolves into tenorite (CuO) in the absence of Zn(II), whereas it transforms into aurichalcite in the presence of Zn(II)

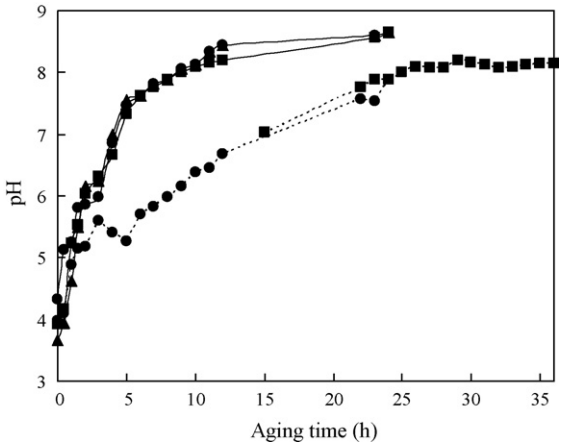

Fig. 4. The pH change of the solution during the homogeneous precipitation using urea. Full line, aged at 90 °C; dotted line, aged at 80 °C. The Cu/Zn/Al composition: (●) 50/50/0; (■) 45/45/10; (▲) 40/40/20.

[18]. It has been established that the *am*-$Cu(OH)_2 \rightarrow CuO$ transformation proceeds *via* a dissolution-reprecipitation mechanism [17]. The same mechanism must operate during the formation of aurichalcite [18].

Actually the precipitates obtained after aging for 2 h at 90 °C showed an intensive reflection around $2\theta = 12.7°$ together with another reflection around $2\theta = 25.6°$, suggesting the formation of highly extended layered structure (Fig. 5). A shoulder observed around $2\theta = 12.0°$ can be assigned to hydrotalcite. Although the two major lines cannot be assigned to any of aurichalcite, malachite and hydrotalcite, the line around $2\theta = 12.7°$ is close to that of aurichalcite, suggesting that this phase is a precursor of aurichalcite $(Cu,Zn)_5(CO_3)_2(OH)_6$, of a low Zn/Cu atomic ratio. ICP analyses of this product showed the atomic ratio of Cu/Zn/Al = 63.6/13.7/22.7, but the analyses of three spots by EDX showed three different atomic ratios of Cu/Zn/Al = 68.7/22.7/8.6, 48.9/28.4/22.7, and 49.0/24.1/26.9, suggesting that the precipitates were not homogeneous. It was reported that aurichalcite structure of the co-precipitate is distorted, causing changes in the XRD pattern, by the incorporation of Al^{3+} during the copreciptation from a solution containing Cu, Zn, and Al nitrates, due to the high charge and acidic nature of Al^{3+} ions compared to those of Cu^{2+} and Zn^{2+} [22]. When the reflection pattern was simulated by replacing one 2e(Cu) site in aurichalcite with Al, the calculated pattern was very close to the pattern of Fig. 5. This clearly suggests that the crystal structure of the precipitate is similar to aurichalcite; probably the precursors of aurichalcite were formed after aging for 2 h.

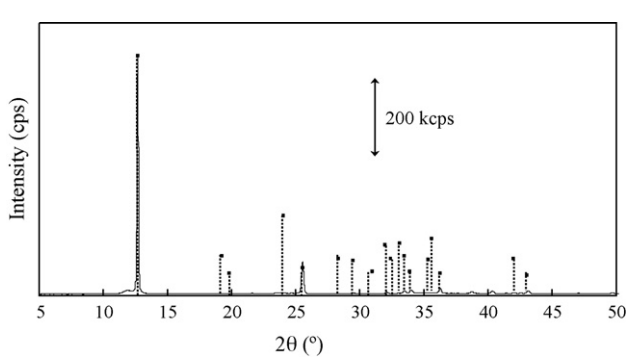

Fig. 5. XRD patterns of the precursors of the *hp*-$Cu/ZnO/Al_2O_3$ (45/45/10) catalysts separated after 3 h of aging at 90 °C (full line) and the reflection pattern simulated by replacing one 2e(Cu) site in aurichalcite with Al (dotted bars).

Usually the homogeneous precipitation by the urea hydrolysis was performed at 90 °C, considering the effective hydrolysis of urea [14–19]. When the aging temperature was decreased to 80 °C, the pH increase became slow compared with that at 90 °C, and reached the final value around 8.0 after aging for 24 h as observed for *hp*-Cu/Zn(50/50) (Fig. 4). Even when the aging time was prolonged up to 36 h, no significant increase was observed in the pH as observed for *hp*-Cu/Zn/Al(45/45/10) (Fig. 4). It is likely that the pH of the solution was mainly controlled by the rate of hydrolysis of urea (Eq. (1)). In all cases, the main component of the final products was aurichalcite, and malachite was detected together with hydrotlcite when Al was added.

3.3. Dissolution of Cu during the precipitation

We have reported that the Cu/Zn binary precursors as-synthesized by aging at 90 °C were composed of aurichalcite single phase of small crystal sizes, and the catalysts after the calcination at 300 °C showed high and stable activity for the shift reaction [14,15]. It is expected that the ternary Cu/Zn/Al system is composed of Zn(Cu)–Al hydrotalcite [23]. However, the presence of Cu^{2+} cations makes the synthetic procedure more complex for two reasons [16]. First, Cu^{2+} ions show the Jahn–Teller effect that favors the formation of distorted octahedral structures and preferentially gives rise to the precipitation of malachite phases. Secondarily, Cu^{2+} ions can be depleted by ammonia originating from urea hydrolysis.

The amounts of Cu and Zn dissolved in the solutions after the separation of the precipitates were determined by the ICP method. The dissolved amounts of both Cu and Zn are shown as both concentration in the solution and percentage in the total amount of metal (Table 2). At 90 °C, the leachings of both Cu and Zn were enhanced with increasing Al content, although the Zn leaching was far smaller than that of Cu. The leaching of Cu exceeded 10% at 20 mol% of the Al content. However, the metal leaching was quite effectively suppressed by decreasing

Table 2
Leaching of Cu and Zn during the catalyst preparation by the *hp*-method

Cu/Zn/Al atomic ratio	Leaching amount[a] (mmol/l)[b]; %[c]			
	Cu		Zn	
	80 °C[d]	90 °C[d]	80 °C[d]	90 °C[d]
50/50/0	0.13; 0.37	1.38; 4.00	0.05; 0.14	0.09; 0.27
45/45/10	0.27; 0.84	3.16; 9.88	0.04; 0.12	0.16; 0.49
40/40/20	0.28; 1.13	3.40; 11.59	0.02; 0.07	0.22; 0.74

[a] Obtained by the ICP analyses of the aqueous solution after the filtration of the precipitates; shown as both concentration in the filtrate.
[b] Percentage in the total metal amount.
[c] For each aging temperature.
[d] The temperature for aging of the precipitates during the *hp*-preparation.

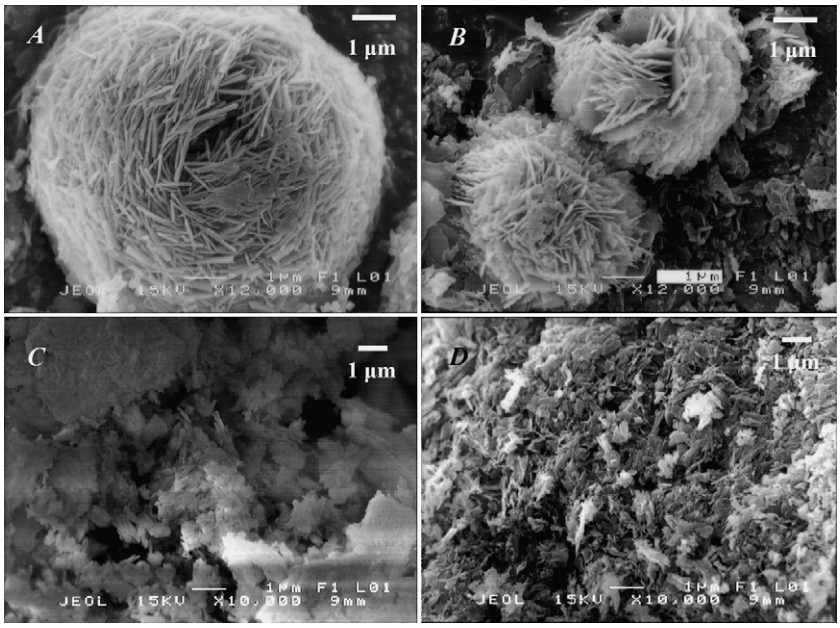

Fig. 6. SEM images of the precursors of the *hp*-Cu/ZnO/Al_2O_3 catalysts. (A) *hp*-Cu/ZnO (50/50) prepared under convection; (B) *hp*-Cu/ZnO/Al_2O_3 (45/45/10) prepared under convection; (C) *hp*-Cu/ZnO (50/50) prepared under stirring; (D) *hp*-Cu/ZnO/Al_2O_3 (45/45/10) under stirring.

the aging temperature from 90 to 80 °C. At 80 °C, the Cu leaching decreased to the value below one-tenth of that at 90 °C; with increasing Al content, however, the Cu leaching still increased and the Zn leaching decreased.

3.4. Effect of the stirring during the precipitation

SEM images of the precursors of the *hp*-Cu/ZnO/Al_2O_3 catalysts are shown in Fig. 6; effect of the stirring of the solution on the morphology of the precursor has been tested. When the *hp*-Cu/ZnO (50/50) and *hp*-Cu/ZnO/Al_2O_3 (45/45/10) were prepared under non-stirring conditions, *i.e.*, under the thermal convection, the precursors showed bird's nest like morphologies composed of large-sized pillar or plate like crystallites (Fig. 6A and B). In contrast, the precursors of *hp*-Cu/ZnO (50/50) and *hp*-Cu/ZnO/Al_2O_3 (45/45/10) prepared under stirring conditions showed quite different morphologies, *i.e.*, agglomerates of rather small-sized crystallites (Fig. 6C and D). In both cases, the sizes of the bird's nest and the crystallites were smaller in the presence of Al than in the absence of Al. These indicate that the crystal growth was much more enhanced under convection than under stirring, and moreover that the co-existence of Al inhibited the crystal growth.

XRD patterns of the precursors of both *hp*-Cu/ZnO (50/50) and *hp*-Cu/ZnO/Al_2O_3 (45/45/10) prepared under convection are shown in Fig. 7. More intensive reflections were observed for both samples compared with those prepared under stirring (Fig. 1A), indicating that the crystal growth was accelerated under the convection coinciding with the results of SEM images (Fig. 6). However, the formation of the malachite phase was also accelerated under the convection even in the absence of Al. It is likely that the malachite formation in cooperation with the enhanced crystal growth caused a decrease in the activity of the *hp*-Cu/ZnO/Al_2O_3 catalysts prepared under the convection.

3.5. Activity of the hp-Cu/ZnO/Al_2O_3 catalysts

The CO conversions in the shift reactions over the *hp*-Cu/ZnO/Al_2O_3 catalysts prepared by aging either at 80 °C or at 90 °C are shown in Fig. 8. The catalysts prepared by aging at 90 °C showed higher CO conversion than those prepared at 80 °C. When the precursor was aged at 90 °C, the CO conversion evidently increased by the addition of 5 mol% of Al and then decreased with increasing Al content to 20 mol%. On the other hand, the CO conversion decreased monotonously with increasing Al content from 0 to 20 mol% by aging at 80 °C. In both cases, the order of the activity well correlated with that of the Cu metal surface area (Table 1).

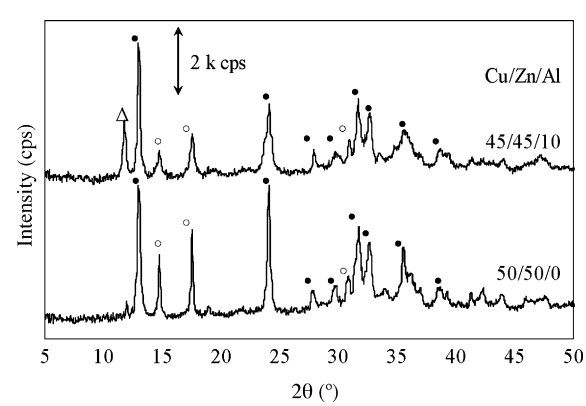

Fig. 7. XRD patterns of the precursors of the *hp*-Cu/ZnO/Al_2O_3 catalysts prepared under convection at 90 °C. (●) Aurichalcite $(Cu,Zn)_5(CO_3)_2(OH)_6$; (▲) hydrotaclite $(Cu,Zn)_6Al_2(OH)_{16}CO_3{\cdot}4H_2O$; (◯) malachite $Cu_2(CO_3)(OH)_2$.

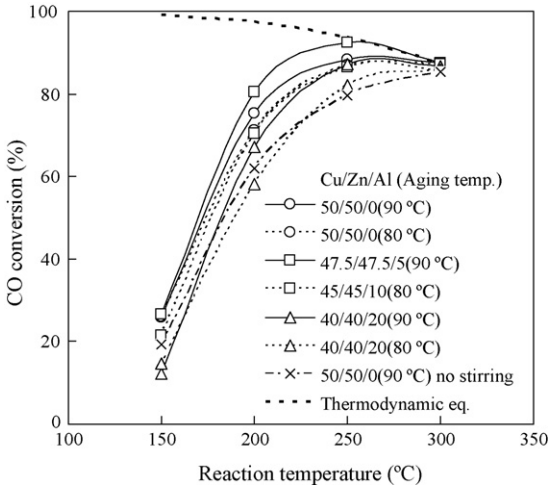

Fig. 8. Activities of the *hp*-Cu/ZnO/Al_2O_3 catalysts prepared by aging at 90 and 80 °C. Catalyst, 100 mg; flow rate: $CO/H_2O/H_2/CO_2/N_2$ = 0.77/2.2/4.46/0.57/30 ml min^{-1}.

We reported previously that the *hp*-Cu/ZnO catalysts showed high and stable activity for the shift reaction [14]. When a large-scale production of the catalysts is considered for the testing in the actual reformer for the PEFC, the aging temperature of 90 °C is too high, since a large amount of steam is produced and a large amount of heat is required. Indeed the *hp*-Cu/ZnO/Al_2O_3 catalysts must be prepared by aging at 80 °C at the highest. Unfortunately the aging at 80 °C caused a slight decrease in the activity as observed for the three *hp*-Cu/ZnO/Al_2O_3 (50/50/0, 45/45/10 and 40/40/20) catalysts (Fig. 8) due to an increasing formation of malachite in the precursors. Malachite is composed of only Cu, whereas aurichalcite is composed of Cu and Zn and formed more selectively at 90 °C than at 80 °C (Fig. 1).

It is reasonable that after the calcination aurichalcite produces CuO/ZnO mixed particles while malachite produces CuO particles alone. Therefore, the former is preferable than the latter for producing finely dispersed Cu metal particles in good contact with ZnO particles. It seems that the formation of aurichalcite as the precursor is indispensable for the formation of the active Cu sites on the catalysts of the low Al content. Millar et al. [24] pointed out an important role of the precursor for Cu/Zn catalysts; the calcination of aurichalcite produced ultimately the most intimately mixed catalyst structure by stabilizing small copper oxide and zinc oxide clusters. It was concluded that the unique formation of an "anion modified" oxide resulting from the initial decomposition stage of aurichalcite was responsible for the "binding" of copper species to zinc moities.

The CO conversion significantly decreased when the *hp*-Cu/ZnO (50/50) catalyst was prepared under the convection *i.e.*, under non-stirring conditions (Fig. 8). This is certainly due to the malachite formation together with the enhanced crystal growth (Fig. 7). It is likely that the former caused a formation of large-sized Cu metal particles from malachite containing Cu as the precursor and the latter also produced large-sized Cu metal particles after the decomposition followed by the reduction.

When the temperature for the reduction pre-treatment was stepwise increased from 200 to 350 °C, the activity showed no substantial decrease up to 250 °C, but the reduction at 350 °C clearly caused a decrease in the activity (data are not shown). It is likely that the reduction of Cu species on the catalyst surface was almost completed by the pre-treatment at 200 °C for 0.5 h on all *hp*-Cu/ZnO/Al_2O_3 catalysts, since no remarkable enhancement was observed in the Cu^0 surface area reduced at 250 °C compared to that at 200 °C. This is also supported by the results of TPR measurements (Fig. 3); all Cu species on the *hp*-Cu/ZnO/Al_2O_3 catalysts were completely reduced at the low temperatures below 300 °C under the TPR conditions. This is in contrast to the results obtained for the *cp*-Cu/ZnO/Al_2O_3 catalysts, on which much higher temperature was required for the reduction of the Cu species (Fig. 3). Steady state reduction of the catalysts at 200 °C for 0.5 h must be enough for the reduction of all Cu species on the *hp*-Cu/ZnO/Al_2O_3 catalysts. The reduction treatment at 350 °C possibly caused a sintering of the Cu metal species on the catalyst surface, resulting in a decrease in the activity. It must be emphasized that the reduction peak around 225 °C was observed as a main peak for all samples irrespective of the Al content (Fig. 3). This low reduction temperature of Cu species around 225 °C is likely to have an important role in the catalytic activity for the CO shift reaction.

3.6. Reducibility of Cu species on the hp-Cu/ZnO/Al_2O_3 catalysts

Fierro and co-workers [25] reported that the Cu/ZnO/Al_2O_3 catalysts prepared by co-precipitation at pH 7.0 and at 70 °C, followed by calcination at 400 °C for 4 h, showed only one reduction peak centered at 223 °C in the TPR, which was assigned to the reduction of CuO to Cu: $CuO + H_2 \rightarrow Cu^0 + H_2O$. The present samples were prepared by the *hp*-method under the varying pH conditions between 4.0 and 8.5 and moreover were calcined under the milder conditions, *i.e.*, at 300 °C for 4 h. Therefore the precursors must differ from those reported by Fierro et al. and the effect of the precursor on the activity must appear more evidently. Although ZnO was not reduced under our experimental conditions, partial reduction of surface ZnO, which may lead to the formation of α-brass (*i.e.*, a dilute alloy of zinc in copper) only a few layers thick on the copper crystallites during the catalyst reduction, cannot be ruled out. In fact, detailed thermodynamic calculations [26] are in favor of such a hypothesis, showing that the equilibrium zinc content in a surface α-brass is about 5% during catalyst reduction at 300 °C.

The shapes of the main reduction peaks centered around 225 °C (Fig. 3), which are asymmetric not only with a tail towards lower temperature but also with shoulders towards higher temperature, may be the result of overlapping of several elemental reduction processes arising from different Cu^{2+} species. The main peak of CuO reduction in the *cp*-Cu/ZnO/Al_2O_3 was displaced by 46 °C towards lower temperatures with respect to that of CuO at 271 °C [25]. This clearly indicates that ZnO enhances the reducibility of the copper phase, which is probably due to the formation of well dispersed CuO particles in contact with the surface of ZnO particles. It has been reported that ZnO promotes the copper reducibility in the overall range of composition of CuO/ZnO binary system [27].

Pettersson and co-workers [28] reported that the reduction of CuO proceeds stepwise ($Cu^{2+} \rightarrow Cu^{+} \rightarrow Cu^{0}$) judging from the TPR results of the Cu/ZnO catalysts impregnated on γ-Al_2O_3; catalysts with 12 wt.% copper loading show two peaks and the second peak may be attributed to the stepwise reduction of copper oxide, which could indicate a strong interaction between part of copper and zinc oxide in the sample. Turco et al. [16] also obtained evidence of the easy reduction of Cu^{2+} to Cu^{+} and Cu^{0} and moreover the formation of stable complexes with Cu^{+} by the CO adsorption measurements on the Cu/ZnO/Al_2O_3 catalysts derived from hydrotalcite precursors. Their precursors were obtained by homogeneous precipitation of metal cations with a properly modified urea method starting from metal chlorides [29]. TPR and TPO measurements indicated that Cu species are easily reduced and reoxidized and Cu^{+} species are intermediate for both processes, and moreover two reduction peaks were observed in the TPR and were related to the two-step reduction: $Cu^{2+} \rightarrow Cu^{+} \rightarrow Cu^{0}$. A two-step reduction of Cu^{2+} was also observed for Cu/ZnO catalysts by the XANES technique [30,31], although in this case the two signals were not distinguished by the TPR technique. In the present work, we observed two or three reduction peaks for each TPR curve, the peak temperatures of which were mainly 225 and 248 °C, and additionally 276 °C for the catalysts of high Al content. It is plausible that the peaks observed at low temperature are assigned to the reduction of Cu^{2+} to Cu^{+}. Actually the reduction peak around 225 °C was observed for all catalysts which revealed the high activity for the shift reaction in the present work. This may be correlated with the fact that Cu^{+} species were observed as the active species by Auger-electron spectra in the previous papers [14,15]. However the amount of H_2 consumed for the reduction of Cu^{2+} to Cu^{+} cannot be quantitatively analyzed in the present TPR measurements, since the peak separation was not good enough and the *hp*-Cu/ZnO/Al_2O_3 catalysts originally contains Cu^{+} in the structure, the amount of which considerably varies depending on the composition and the preparation procedure. Moreover each peak cannot be strictly assigned to the reduction of either Cu^{2+} to Cu^{+} or Cu^{2+} to Cu^{0}. Further careful and extensive studies will be required for the correct evaluation of the amount of Cu^{+}.

3.7. Turnover frequency of the hp-Cu/ZnO/Al_2O_3 catalysts

Turnover frequencies (TOF) of the *hp*-Cu/ZnO/Al_2O_3 catalysts were calculated from the CO conversion at 150 °C based on the surface Cu metal and plotted against the Al content (Fig. 9). The TOFs values obtained over the *hp*-Cu/ZnO/Al_2O_3 catalysts were higher than those obtained over the *cp*-Cu/ZnO/Al_2O_3 catalysts as references. These *cp*-Cu/ZnO/Al_2O_3 catalysts were prepared by the co-precipitation method at pH 9.0 using NaOH as the pH controller, which was the best conditions for preparing the *cp*-catalysts [32]. The TOFs of the *hp*-Cu/ZnO/Al_2O_3 catalysts were high for the Al content below 10 mol%, but decreased with further increasing Al content up to 20 mol%. This well correlated with the dependence of the TPR peak intensity around 225 °C on the Al content for the *hp*-Cu/ZnO/Al_2O_3 catalysts (Fig. 3). The TOFs of the *hp*-Cu/ZnO/Al_2O_3 catalysts prepared

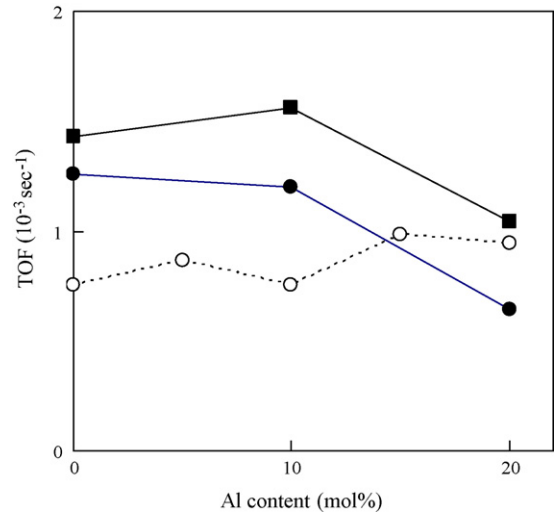

Fig. 9. Turnver frequency of the *hp*-Cu/ZnO/Al_2O_3 catalysts prepared by aging at 90 °C (●) and 80 °C (■). (◯) *cp*-Cu/ZnO/Al_2O_3 catalysts as reference (prepared by precipitation at pH 9.0 with NaOH as the pH controller).

by aging at 80 °C were higher than those prepared by aging at 90 °C. The results obtained above clearly suggest that the active sites cannot be identified as metallic Cu species. The nature of the Cu active site varies depending on the Al content and the preparation method of the Cu/ZnO/Al_2O_3 catalysts.

3.8. Active sites on the hp-Cu/ZnO/Al_2O_3 catalysts

We reported that the real active species on the *hp*-Cu/ZnO catalysts are not Cu^{0} but Cu^{+} formed on the catalyst surface, since the TOF dependence on the Cu/Zn composition became more constant when they were calculated based on the surface amount of Cu^{+} than that of Cu^{0} both estimated from Auger-electron spectra [14,15]. The Auger-electron spectra also clearly indicated *in situ* oxidation of Cu^{0} to Cu^{+} in the presence of steam at room temperature, suggesting that the reduction–oxidation between Cu^{0} and Cu^{+} promoted the shift reaction (Eqs. (2) and (3)) and the reaction (3) must be the

$$2Cu^{0} + H_2O \rightarrow Cu_2{}^{+}O + H_2 \quad (2)$$

$$Cu_2{}^{+}O + CO \rightarrow 2Cu^{0} + CO_2 \quad (3)$$

rate-determining step [14,15].

There are various theories describing the nature of Cu–ZnO interactions in the catalyst [33]. For instance, some authors have suggested that Cu is incorporated in the ZnO phase on interstitial and substitutional sites, assuming three possible valence states (Cu^{0}, Cu^{+} and Cu^{2+}) [34,35]. XPS measurements revealed the existence of Cu^{+} species on the surface of binary Cu/ZnO catalysts prepared *via* hydroxycarbonate precursors in aqueous solution after exposure to an O_2/CH_3OH mixture [36]. It was reported that ZnO segregates after reduction of Cu/ZnO/SiO_2 catalysts; the migration of ZnO on top of Cu was followed by the formation of a (partly) oxidized Cu in a Cu^{+}/ZnO surface with oxygen vacancies which worked as the active sites for methanol synthesis [37]. As for the shift reaction, it was reported that the

reaction was catalyzed *via* a reduction–oxidation mechanism between $Cu^0 \leftrightarrow Cu^+$, in which Cu^+ sites chemisorbed and oxidized CO to CO_2 to form Cu^0, whereas the reduced Cu^0 sites were reoxidized by H_2O to form Cu^+ and H_2 [38,39]. None the less, the important role Cu^0 cannot be excluded since the reaction proceeded by the reduction–oxidation mechanism between Cu^0 and Cu^+. Moreover, the amount of Cu^+ sites reasonably depends on the particle size of Cu metal if Cu^+ forms at the boundary between Cu metal particles and ZnO particles, suggesting an apparent dependence of the activity on Cu^0 species.

Indeed the addition of only small amount of Al_2O_3 afforded better catalytic performance for the binary Cu/ZnO catalysts (Fig. 8). Actually ternary $Cu/ZnO/Al_2O_3$ catalysts have been used in the reformer. No clear evidence was obtained for explaining the role of Al_2O_3 in the ternary $Cu/ZnO/Al_2O_3$ catalysts in the present work. It is expected that Al_2O_3 can work as a binder between Cu and ZnO or a stabilizer of the active Cu metal species.

4. Conclusions

The $Cu/ZnO/Al_2O_3$ catalysts were prepared by homogeneous precipitation (*hp*), and the effects of the Al component on the catalysts precursors and further on the catalytic activity for the water-gas shift reaction were studied. During the precipitation, Cu(II) nitrate was first hydrolyzed at low pH, followed by the hydrolysis of Zn(II) nitrate with increasing pH; amorophous $Cu(OH)_2$ formed first was converted to the final Cu/Zn bimetallic product, *i.e.*, aurichalcite, *via* a dissolution-reprecipitation mechanism assisted by Zn(II). During the *hp*-preparation, a significant Cu leaching was observed, but was effectively suppressed by lowering the aging temperature from 90 to 80 °C. A main crystal phase in the precursor was always Cu/Zn bimetallic aurichalcite, and malachite and hydrotalcite appeared as contaminants with increasing Al content. The formation of malachite caused a lowering in the activity probably due to its monometallic Cu property. Only an addition of small amount of Al on the Cu/ZnO binary catalyst was effective for the activity enhancement and the further addition caused a decrease not only in the specific surface area but also in the Cu metal surface area, resulting in a decrease in the catalytic activity. The activity apparently depended on the Cu metal surface area of *hp*-catalysts, but TOF varied significantly depending on the preparation method as well as on the Al content. The *hp*-catalysts showed higher TOFs values than the *cp*-catalysts. It is likely that the active sites are composed of Cu^+ species obtained by the $Cu^{2+} \rightarrow Cu^+$ reduction around 225 °C as observed in the TPR measurements. An important role of Cu/Zn bimetallic aurichalcite as the catalyst precursor and reduction–oxidation between Cu^+ and Cu^0 as the catalytic mechanism of the shift reaction has been suggested.

Acknowledgement

The authors gratefully acknowledge Prof. Hiroshi Fukuoka, Department of Chemistry and Chemical Engineering, Hiroshima University, for his helpful suggestions in determining crystal structure of the intermediates.

References

[1] G.G. Scherer, Solid State Ionics 94 (1997) 249.
[2] S. Ahmed, M. Krumpelt, Int. J. Hydrogen Energ. 26 (2001) 291.
[3] V.M. Schmidt, P. Bröcheerhoff, B. Höhlein, R. Menzer, U. Stimming, J. Power Sources 49 (1994) 299.
[4] F. Vidal, B. Busson, C. Six, O. Pluchery, A. Tadjeddine, Surf. Sci. 502/503 (2002) 485.
[5] M.J.L. Ginés, N. Amadeo, M. Laborde, C.R. Apesteguía, Appl. Catal. A 131 (1995) 283.
[6] Y. Tanaka, T. Utaka, R. Kikuchi, K. Sasaki, K. Eguchi, Appl. Catal. A 238 (2003) 11.
[7] M. Rønning, F. Huber, H. Meland, H. Venvik, D. Chen, A. Holmen, Catal. Today 100 (2005) 249.
[8] K. Sekizawa, S. Yano, K. Eguchi, H. Arai, Appl. Catal. A 169 (1998) 291.
[9] T. Utaka, K. Sekizawa, K. Eguchi, Appl. Catal. A 194/195 (2000) 21.
[10] Y. Tanaka, T. Utaka, R. Kikuchi, K. Sasaki, K. Eguchi, Appl. Catal. A 242 (2003) 287.
[11] Y. Tanaka, T. Utaka, R. Kikuchi, T. Takeguchi, K. Sasaki, K. Eguchi, J. Catal. 215 (2003) 271.
[12] Y. Tanaka, T. Takeguchi, R. Kikuchi, K. Eguchi, Appl. Catal. A 279 (2005) 59.
[13] T. Shishido, Y. Yamamoto, H. Morioka, K. Takaki, K. Takehira, Appl. Catal. A 263 (2004) 249.
[14] T. Shishido, M. Yamamoto, D. Li, Y. Tian, H. Morioka, M. Honda, T. Sano, K. Takehira, Appl. Catal. A 303 (2006) 62.
[15] T. Shishido, M. Yamamoto, I. Atake, D. Li, Y. Tian, H. Morioka, M. Honda, T. Sano, K. Takehira, J. Mol. Catal. A 253 (2006) 270.
[16] M. Turco, G. Bagnasco, U. Constantino, F. Marmottini, T. Montanari, G. Raims, G. Busca, J. Catal. 228 (2004) 43.
[17] R.J. Candal, A.E. Regazzoni, M.A. Blesa, J. Mater. Chem. 2 (1992) 657.
[18] G.J. de, A.A. Soler-Illia, R.J. Candal, A.E. Regazzoni, M.A. Blesa, Chem. Mater. 9 (1997) 184.
[19] H. Morioka, H. Tagaya, K. Karasu, J. Kadokawa, K. Chiba, J. Solid State Chem. 117 (1995) 337.
[20] J.W. Evans, M.S. Wainwright, A.J. Bridgewater, D.J. Young, Appl. Catal. 7 (1983) 75.
[21] C.F. Baes, P.E. Mesmer, The Hydrolysis of Cations, John Wiley, New York, 1976.
[22] G. Sengupta, R.K. Sharma, V.B. Sharma, K.K. Mishra, M.L. Kundu, R.M. Sanyal, S. Dutta, J. Solid State Chem. 115 (1995) 204.
[23] F. Cavani, F. Trifiro, A. Vaccari, Catal. Today 11 (1991) 173.
[24] G.J. Millar, I.H. Holm, P.J.R. Uwins, J. Drennan, J. Chem. Soc. Faraday Trans. 94 (1998) 593.
[25] I. Melián-Cabrera, M. López Granados, J.L.G. Fierro, J. Catal. 210 (2002) 273.
[26] M.S. Spencer, Surf. Sci. 192 (1987) 323, 329, 336.
[27] G. Fierro, M. Lo Jacono, M. Inversi, P. Porta, F. Cioci, R. Lavecchina, Appl. Catal. A 137 (1996) 327.
[28] B. Lindström, L.J. Pettersson, P.G. Menon, Appl. Catal. A 234 (2002) 111.
[29] U. Constantino, F. Marmottini, M. Nocchetti, R. Vivani, Eur. J. Inorg. Chem. (1998) 1439.
[30] T.L. Reitz, P.L. Lee, K.F. Czaplewski, J.C. Lang, K.E. Popp, H.H. Kung, J. Catal. 199 (2001) 193.
[31] M.M. Günter, T. Ressler, B.E. Jentoft, B. Bems, J. Catal. 203 (2001) 133.
[32] K. Nishida, I. Atake, D. Li, T. Shishido, Y. Oumi, T. Sano, K. Takehira, submitted.
[33] M.M. Günter, T. Ressler, B. Bems, C. Büscher, T. Genger, O. Hinrichsen, M. Muhler, R. Schlögl, Catal. Lett. 71 (2001) 37.
[34] K. Klier, Adv. Catal. 31 (1982) 243.
[35] V. Ponec, Surf. Sci. 272 (1992) 111.
[36] J. Agrell, M. Boutonnet, I. Melián-Cabrera, J.L.G. Fierro, Appl. Catal. A 253 (2003) 201.
[37] W.P.A. Jansen, J. Beckers, J.C.v.d. Heuvel, A.W. Denier v.d. Gon, A. Bliek, H.H. Brongersma, J. Catal. 210 (2002) 229.
[38] Y. Li, Q. Fu, M. Flytzani-Stephanopoulos, Appl. Catal. B 27 (2000) 179.
[39] N.A. Koryabkina, A.A. Phatak, W.F. Ruettinger, R.J. Farrauto, F.H. Ribeiro, J. Catal. 217 (2003) 233.